Turkish Computational and Theoretical Chemistry

Turkish Comp Theo Chem (TC&TC)

Volume(Issue): 9(2) – Year: 2025 – Pages: 52-65

e-ISSN: 2602-3237

https://doi.org/10.33435/tcandtc.1506442

Received: 29.06.2024 ***Accepted***: 21.08.2024 *Research Article*

Virtual Screening Bioactive Compounds of Rheum Genus in Inhibiting Steatohepatitis: In silico studies

Ahmad[a, 1], Firdayani[b], Irma Ratna Kartika[a]

[a]Chemistry Study Program, Faculty of Mathematics and Natural Sciences, Jakarta State University (UNJ), Jakarta, Indonesia

[b]Research Center for Vaccine and Drugs, Research Organization for Health, National Research and Innovation Agency (BRIN), South Tangerang Indonesia

Graphic abstract

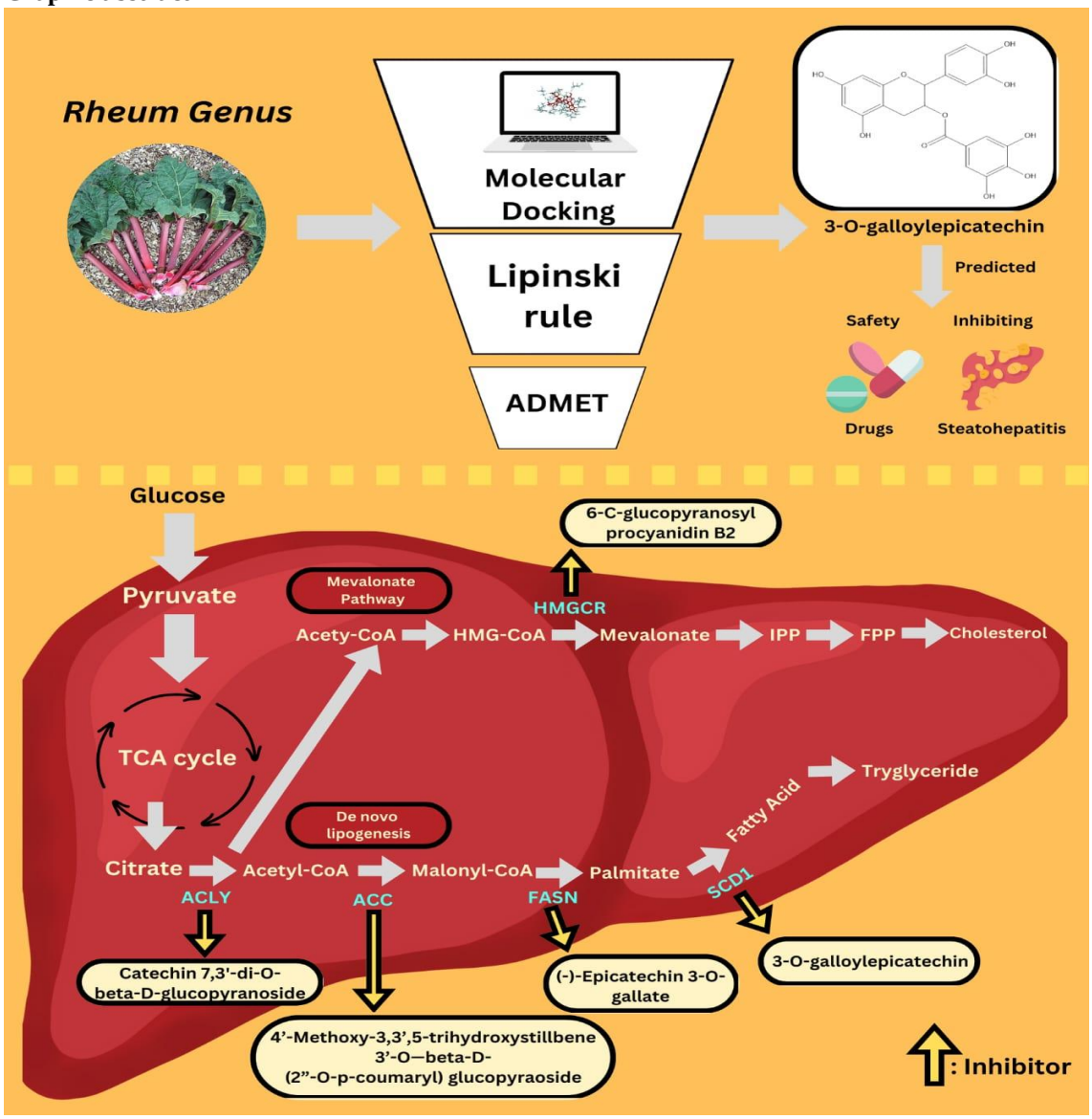

[1] Corresponding Authors

e-mail: ahmaddachyar@gmail.com

Abstract: The fatty liver disease known as steatohepatitis is characterized by liver inflammation. De novo lipogenesis and mevalonate pathway have been identified as contributing to the development of fatty liver. Rheum genus has pharmacological properties such as antioxidant, anti-inflammatory, hepatoprotective, and hypolipidemic. Consequently, the current study investigated bioactive compounds from Rheum genus using in-silico method. The 109 compounds and their natural inhibitors against the enzyme targets ATP-citrate lyase (ACLY), Acetyl-CoA carboxylase (ACC), Fatty Acid Synthase (FASN), Stearoyl-CoA desaturase (SCD1), and HMG-CoA reductase (HMGCR) were performed. The results obtained are in the form of a re-rank score, with the best compound results for each enzyme is Catechin 7,3'-di-O-β-D-glucopyranoside (A1) (-148.73), 4' - Methoxy - 3, 3',5 - trihydroxystilbene' - O - β – D (2''-O-p-coumaryl) - glucopyranoside (A2) (-136,808), 2-Cinnamoyl-1,6-digalloyl glucose (A3) (-149,589), 3-O-Galloyl Epicatechin (A4) (-160,018), and 6-C-Glucopyranosyl Procyanidin B2 (A5) (-84,843) as ACLY, ACC, FASN, SCD1 and HMGCR inhibitors, respectively. Analyses using the ADMET and Lipinski rules revealed that A4 has the potential to be a lead compound for oral drug use, but more research is required.

Keywords: Fatty liver, de novo lipogenesis, mevalonate pathway, rheum genus, in-silico.

Highlight

- Steatohepatitis is a disorder in which the liver is inflamed and fat accumulates (steatosis). It indicates a more advanced stage of fatty liver disease, in which simple fat buildup leads to inflammation and liver cell damage.
- *Rheum* is a genus of plants in the Polygonaceae family that includes numerous species usually known as *rhubarb.* Its bioactives exhibit antioxidant and anti-inflammatory properties.
- An in-silico study is research that uses computer simulations or computational models.

1. Introduction

The liver regulates fatty acid and cholesterol metabolism, and disruptions in intrahepatic activity can affect metabolic health [1]. Each year, around two million people suffer deaths from liver disease. Fatty liver disease is developing worldwide and is predicted to be a factor in liver transplantation by 2030. Extra fat in the liver is a risk factor for developing liver disease [2,3]. Non-alcoholic fatty liver disease (NAFLD) is an early-stage liver disease that requires inflammation or intake of alcohol. Non-alcoholic steatohepatitis (NASH) is a more advanced type of hepatocyte inflammation [4]. This is due to its tight correlation with other metabolic diseases, such as type 2 diabetes, in which about 75% of the population has liver fat accumulation [5].

De novo lipogenesis (DNL) is a process of metabolism in the liver that produces fatty acids from glucose. Excessive development of this pathway contributes to the accumulation of fat in the liver [6,7]. Inhibiting DNL enzymes such as ACLY, ACC, FASN, and SCD1 activity can reduce fat accumulation in the liver [8,9]. There are multiple inhibitors of these DNL enzymes, such as NDI-091143, ND-646, TVB-2640, and aramchol, respectively. The mevalonate pathway is an essential process in cholesterol synthesis. Inhibiting mevalonate pathway enzymes such as 3-hydroxy-3-methylgluratyl coenzyme-A reductase (HMGCR) can reduce cholesterol biosynthesis, making it a primary target for cholesterol-lowering medications, such as statins [10]. However, statins can improve liver serum and induce muscle pain [11].

The Rheum genus contains the most beneficial substances. In recent years, scientific and clinical studies have revealed various biological effects in Rheum genus plants [12]. These effects include hypolipidemic, antimicrobial, anti-inflammatory, and antioxidant properties. Rhubarb is a plant belonging to the Rheum genus. The pharmacological of Rhubarb can lower serum triglyceride levels and liver steatosis [13]. The roots of Rheum emodi have been shown to perform hepatoprotective and antioxidant activities [14]. Rheum officinale Baill is also reputed to have hepatoprotective bioactivity [15]. Rheum turkestabucyn rhizome extract can decrease serum triglyceride and has antioxidant activities [16]. The discovery of several Rheum species plants with the

potential for reducing fatty liver led to research into the Rheum genus bioactive compounds.

Virtual screening has been a standard assay in drug development [17]. Molecular docking also aims to find the most stable conformation of protein and ligand, then analyze the docking complex that gives the lowest re-rank score to predict the interaction and the resulting energy [18]. The requirements for a good drug are that it must be easily absorbed by the body and bind to target molecules, such as proteins. These properties are called ADMET (absorption, distribution, metabolism, elimination, toxicity). The principle commonly used is the Lipinski rule of five, which looks at molecular weight, donor-acceptor H-bonds, and Log P [19].

In this study, we used virtual screening molecular docking to examine the potential of the Rheum genus bioactive compounds based on the re-rank score as inhibitors of steatohepatitis. After that, the Lipinski rule of five and ADMET were tested to see if the compound could be used as an oral drug predicted to inhibit de novo lipogenesis and mevalonate pathway.

2. Computational Method

The website www.knapsackfamily.com provided information on 109 Rheum compounds. The resources utilized in this work were 3D structures of the enzymes ACLY (PDB ID: 6O0H), ACC (PDB ID: 5KKN), FASN (PDB ID: 8GKC), SCD1 (PDB ID: 4ZYO), and HMGCR (PDB ID: 1HW9) obtained from the website https://www.rscb.org. Molegro Virtual Docker 6.0.0 was used for molecular docking, and the Discovery Studio 2024 client was used for compound visualization. ADME and toxicity were tested using the websites www.swissADME.com and www.scfbio-iitd.res.in , respectively.

2.1. Enyzmes and ligand preparation

The three-dimensional (3D) structures of enzymes utilized in the study were retrieved from https://www.rscb.org and stored in PDB format. The enzymes were isolated by eliminating water and cofactors from the protein structure. The ligands' 3D structure was modeled using the ChemOffice software tool (PerkinElmer) and optimized for energy using the Merck molecular force field 94 (MMFF94), saved in mol2.format [20].

2.2. Molecular Docking Simulation

First, the molecular docking study is validated by re-docking the enzymes with the natural ligand. Based on the literature, we determined the chain structure and native ligand to use. Grid Box Docking can enhance the docking process time while decreasing the selectivity of docking on specific target pocket binding sites [21]. After validation, docking of the developed test ligand was done. The test ligand is added to the program, and alignment is performed with the reference ligand. Following that, docking simulations were run on each chemical, which was then changed into active ligands (set as active ligands), and the results were examined. Docking results were visualized using Discovery Studio, amino acid interactions were analyzed, and scores were re-ranked.

2.3. Lipinski and ADMET properties calculations

The structure of the five compounds from the Rheum genus with the highest re-rank score for each enzyme was investigated further using the ADMET and Lipinski rule of five. SWISSADME assessed the compounds physicochemical limitations, pharmacokinetics, and drug-likeness. In addition, the toxicity prediction for oral administration was calculated using Protox II (tox.charite.de). This toxicity prediction is used to analyze hepatotoxicity and cytotoxicity [22]. This toxicity prediction helps assess hepatotoxicity and cytotoxicity. Following that, the Lipinski Rule of Five test was performed.

3. Results and discussion

3.1. Validation methods

First, validation docking or re-docking is performed, and the native ligand is tethered to the protein binding site. Grid size and radius obtained via re-docking were employed as a reference for the docking stage of the compound of the Rheum genus. RMSD is the similarity of two atomic coordinates used for docking validation [23]. An RMSD value of less than 2 Å is considered acceptable. The smaller the RMSD, the closer the ligand site is to its original form [24]. In table 1. The re-docking results are < 2 Å, except for SCD1, which has an RMSD value of 3.2 Å. This refers to the complicated structure of SCD1's native ligand, Stearoyl-CoA, which has a long carbon chain and

is difficult to position in its native conformation, as well as the unpredictability of its structure.

3.2. Virtual screening of *Rheum* genus

Flavonoid and phenolic compounds that inhibit lipogenesis enzymes can decrease the evolution of steatohepatitis by reducing inflammation, oxidative stress, and lipid metabolism [25,26]. Following *re-docking* and compound collection, docking was applied to these compounds. This docking generates a *re-ranking* score. The *re-rank* score is a figure that reflects the bond energy required to form a bond with the enzymes, from which the activity or compound can be anticipated. To see and select the best inhibitor from the *Rheum* genus, molecular docking was performed on the specific active site of the enzymes. The lower the *re-rank* score, the stronger the bonding connection between the ligand and the protein [27].

Table 1. Validation Docking and Grid Box

Enzyme	PDB Code	Radius	Center Grid Box	RMSD
ACLY	6O0H	15	X: 128.27 Y: 156.19 Z: 182.66	0.8 Å
ACC	5KKN	10	X: 54.00 Y: 38.96 Z: 43.99	1.1 Å
FASN	8GKC	15	X: 105.78 Y: 180.15 Z: 133.21	1.1 Å
SCD1	4ZYO	15	X: 17.43 Y: 70.83 Z: 47.03	3.2 Å
HMGCR	1HW9	15	X: -12.68 Y: -28.69 Z: 22.65	1.3 Å

Table 2. Docking Results Between Enzyme and Compounds

Enzyme	Compound	*Re-rank* score	Conventional Hydrogen Bond
ATP-citrate lyase PDB ID: (6O0H)	NDI-091143	-126.569	**Gly380,** Thr353, Arg378, Gly380
	Bempedoic Acid	-97.358	**Gly380**
	A1	-148.731	Ala280, Gly309, Ala310, Ile344, Asn349, Asn346, Met278, Gly342, **Gly380,** Arg378, Asn346
Acetyl-CoA carboxylase PDB ID: (5KKN)	ND-646	-145.16	Arg277
	Firsocostat	-98.854	**Arg281**
	A2	-136.808	**Arg281,** Trp681, Asn679, Phe704, Pro590, Glu671, Glu593
Fatty Acid Synthase PDB ID: (8GKC)	TVB-2640	-89.489	-
	Orlistat	-92.552	Ser2081, Asn2028, **Asn2028**
	A3	-149.589	Ile2079, **Asn2028**, Gln2031, Asp1977, Ser2023, Thr2083, Asn2028
HMG-CoA reductase PDB ID: (1HW9)	Simvastatin	-68.440	Asn755, **Glu559**
	A5	-84.843	Ala751, **Glu559,** Glu559, Gly560, Ala856,

In table 2. shows some compounds such as native ligands, compounds that have been determined as inhibitors clinical of each enzyme, and docking results of rheum genus compounds with the highest re-rank score targeted at each enzyme ACLY, ACC, FASN, SCD1, and HMGCR. Compound A1 is found in Rhubarb from Rheum palmatum, R.officinale, and Rheum rhaponticum [28]. Compound A2 was discovered in Rhubarb from Rheum rhaponticum [29]. The roots of the Rhubarb-type Rheum officinale contained compound A3 [30]. Compound A4 is found in Rhubarb from Rheum tanguticum [31]. Compound A5 is also found in Rhubarb from the epidermis of

Cinnamomum cassia and C.abtusi folium [32]. Flavonoid compounds and stilbene glycosides are among the five compounds. Based on docking results of 109 compounds in each enzyme, it can be determined that flavonoid glycoside compounds always present and have the best re-rank score are catechin-5,3'-di-O-β-D-glucopyranoside. Catechin glycosides include catechin-7,3'-di-O-β-D-glucopyranoside, catechin - 3,4' – di – O – β – D-glucopyranoside, catechin – 5 – O – β – D - glucopyranoside, 7-O-β-D-glucopyranosylcatechin. Catechin glucopyranoside is a flavonoid compound of the flavan-3-ol group bound to glycosides. Flavan-3-ols exert their antioxidant effects [33]. In the report, Catechin-5-O–β-D-glucoside from Bauhinia pentandra showed anti-inflammatory activity with an inhibition rate of over 33.0% ± 4.0 [34]. 7-O-β-D-glucopyranosylcatechin isolated from the seed of Phaseolus calcaratus has beneficial roles in the scavenging of ROS and treatment of oxidative stress [35]. (+)-Catechin 3-O-β-D-glucopyranoside isolated from Trichilia emetica whole seeds has beneficial antioxidant activity at 80% DPPH % inhibition [36]. Flavonoid glycosides have antioxidant properties that may counteract hepatic fat accumulation by activating the PPAR-α-FGF21-AMPK-PGC-1α signaling cascade associated with DNL reduction [37]. There have been no further study reports for the other top-ranked substances.

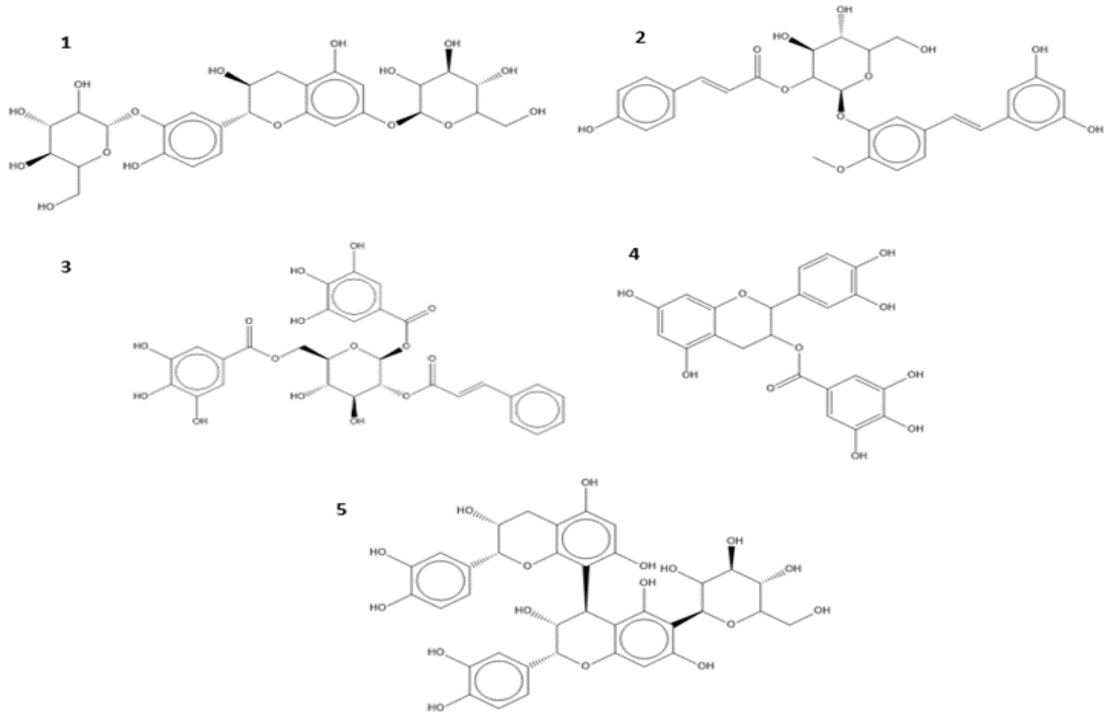

Figure 1. Structure of the compound with the lowest bond energy (1) Catechin 7,3’ di-O-β-glucopyranoside (A1), (2) 4’–methoxy–3,3’,5-trihydroxystilbene 3’–O–β–D-(2-O-p-coumaryl)–glucopyranoside (A2), (3) 2–cinnamoyl-1,6–digalloylglucose(A3),(4)3–O-galloylepicatechin(A4), (5) 6 – C - glucopyranosylprocyanidin B2 (A5).

Enzyme ACLY generates acetyl-CoA and oxaloacetate which is a key lipogenesis regulator and is considered a therapeutic target for the treatment of hyperlipidemia since it can impact lipid and cholesterol production [38][39]. The re-rank score of A1 with ACLY is -148.731, while those for NDI-091143 and bempedoic acid is -126.569 and -97.358, respectively. NDI-091143 is a compound that bind allosterically to the ACLY enzyme and forms a hydrogen bond with Gly380 and is effective in inhibiting ACLY enzyme function [40]. Bempedoic acid is a prodrug that is converted to an active form ETC-1002 CoA by acyl-CoA synthetase and is known to affect adenosine monophosphate-activated protein kinase (AMPK) activation and ATP citrate lyase (ACLY) inhibition [41]. The docking result compound, a flavonoid glycoside compound on ACLY enzyme,

is catechin. Catehin-5-O-β-glucopyranoside with re-rank score -131.005. It can be predicted that the Catehin-5-O glucopyranoside compound has better binding energy than NDI-091143 and Bempedoic acid, so A1 and Catehin-5-O-glucopyranoside, predicted that can inhibit ACLY.

Enzyme ACC catalyzes the carboxylation of acetyl-CoA and produces malonyl-CoA [42]. Targeting this ACC enzyme may decrease de novo fatty acid, which is linked to NASH, diabetes, and other metabolic disorders [43]. Previous research found that the ACC inhibitor firsocostat reduced hepatic DNL after 4 and 12 weeks, using a residual label correction approach that accounts for hepatic triglyceride turnover [44]. A2 with ACC was compared to the ND-646 and firsocostat with re-rank score of -145.16, -98.854, and -136.808, respectively. The A2 re-rank score is higher than Firsocostat but slightly lower than the ND-646. ND-646 is an allosteric inhibitor of ACC that has a distinctive mechanism of action. It binds to the BC domain of ACC, where the AMPK phosphorylation serine of ACC interacts to prevent ACC dimerization and activation [45]. Firsocostat is a liver-targeted, small molecule allosteric inhibitor of both ACC1 and ACC2 that binds to the BC domain, preventing dimerization and reducing enzyme activity [46]. This might show that A2 has a high capacity to inhibit ACC. The flavonoid glycoside compound with a good re-rank score on the ACC enzyme is Catechin 5,3'-di-O-β-D-glucopyranoside with a re-rank score of -134.752. This result is higher than ND-646 and Firsocostat but lower than A2.

The enzyme FASN converts malonyl-CoA to palmitate. Palmitate generated by FASN has numerous potential destinations in the liver of persons with NAFLD since it is a building block for synthesizing fatty acids and more complex lipids, such as triglycerides, which induce steatosis. FASN catalyzes fatty acid synthesis. In a previous study, FASN inhibition acted directly on the primary cell types of NASH [47][48]. A3 with FASN has a higher re-rank score than the TVB-2640 and orlistat, which is -149.589. TVB-2640 is a small-molecule human FASN inhibitor. TVB-2640 is the first highly selective FASN inhibitor to reach clinical trials [49]. Orlistat is a new inhibitor of the thioesterase domain of fatty acid synthase [50]. The lower re-rank score, the higher the binding energy. A3 is anticipated to inhibit the FASN enzyme more effectively than the TVB-2640 and Orlistat. The best flavonoid glycoside compounds from FASN enzyme docking results are Catechin 5,3'-di-O-β-D-glucopyranoside and Catechin 3'-O-β-D-glucopyranoside with a re-rank score -147.059 and -141.006. These results predict that these flavonoid glycoside compounds have better inhibitory activity than orlistat and TVB-2640.

Enzyme SCD1 is a lipid biosynthesis stimulant that produces new phospholipids for cell membrane biogenesis by converting palmitic acid to palmitoleic acid. Aramchol has been shown in a prior study to decrease SCD1 and enhance PPARG mRNA expression, which may have antifibrotic effects in individuals with NASH and fibrosis [51][52]. Stearoyl-CoA is a substrate that can be the active binding site of SCD1. Stearoyl-CoA is a substrate that can be the active binding site of SCD1 [53]. Aramchol is a drug currently in clinical trials for fatty liver disease that works to suppress the SCD1 enzyme thereby reducing the expression of genes and proteins associated with liver fibrosis [54]. A4 with SCD1 has a high ability to inhibit the SCD1 enzyme. Flavonoid glycoside compounds that have the best docking results against the SCD1 enzyme are catechin 5,3'-di-O-β-D-glucopyranoside and catechin 5,4'-di-O-β-D-glucopyranoside with re-rank score -157,225 and -150,285. These results predict that these compounds have better inhibitory activity than native ligand and aramchol. A4 has a strong and substantial re-rank score of -160.018, whereas the Stearoyl-CoA and aramchol have scores of -70.023 and -78.004, respectively.

De novo lipogenesis and lipid metabolism in the liver can be targeted to minimize fatty livers. The imbalance in triglyceride (TG) synthesis can be used to predict fat gain. DNL products, which are fatty acyl chains connected to coenzyme A, can accumulate and be integrated into various of lipids. Lipids perform a metabolic function and can be harmful if DNL levels grow [55].

The function of the enzyme HMGCR is to prevent HMG-CoA from converting mevalonate acid, the primary substrate for cholesterol synthesis, which can lead to inflammation and fatty liver. These pathways cause the liver to accumulate cholesterol, which may lead to inflammation and hepatocellular death [56][57]. A5 with HMGCR has a higher re-

rank value of -84.843 than the native ligand, which is -68.440. This suggests that compound A5 has more inhibitory efficacy than its native ligand (simvastatin). Flavonoid glycoside compounds that have the best docking results on HMGCR enzyme are Catechin 5,3'-di-O-β-D-glucopyranoside and 7-O-β-D-Glucopyranosylcatechin with re-rank score -77.4605 and -76.7536. These results predict that these compounds have better inhibitory activity than the simvastatin.

The mevalonate pathway generates isoprenoids, which are required for various cellular processes ranging from cholesterol synthesis to growth control. The enzyme 3-hydroxy-3-methylglutaryl-coenzyme A reductase (HMGCR), which converts HMG-coenzyme A to mevalonate, is the rate-limiting enzyme in the mevalonate pathway [58].

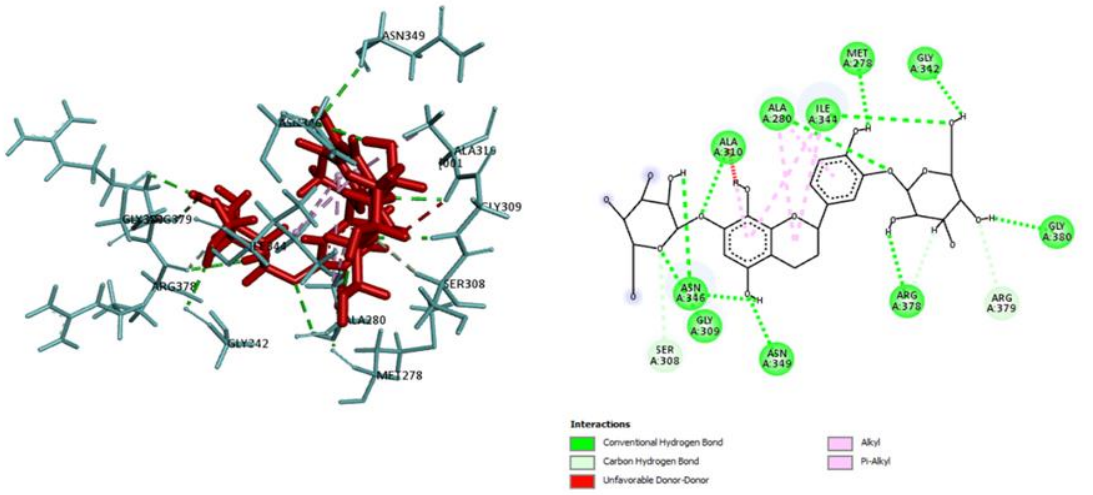

Figure 2. 2D and 3D ligand (A1)-target interactions at binding site of ACLY (6O0H)

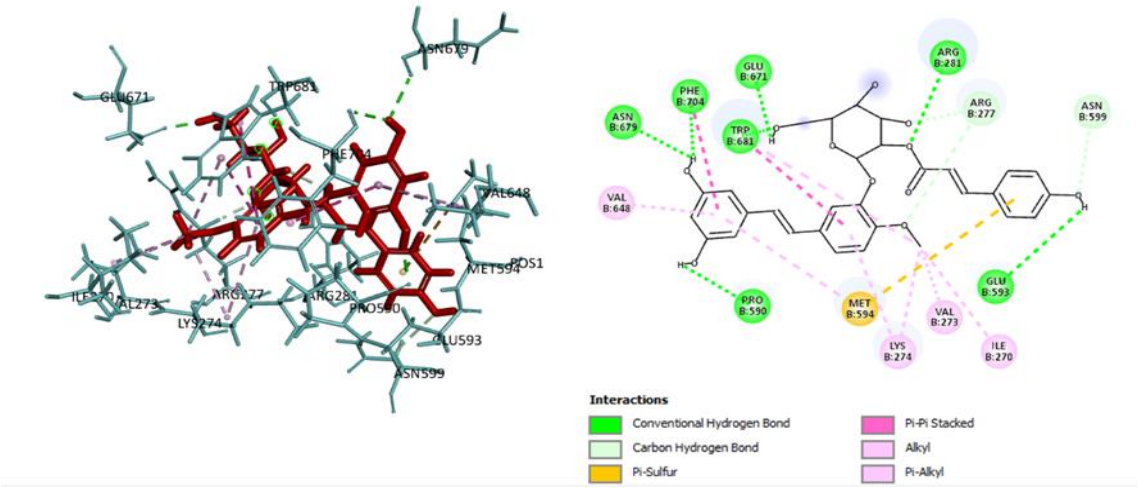

Figure 3. 2D and 3D ligan (A2)-target interactions at binding site of ACC (5KKN)

A1 binding ACLY forms 14 hydrogen bonds with ALA280, GLY309, ALA310, ILE344, ASN349, ASN346, MET278, GLY342, GLY380, ARG378, ASN346, SER308, ARG379, and ARG378 at distances of 2.78, 2.24, 2.19, 2.21, 2.59, 2.32, 2.09, 2.15, 2.18, 2.62, 2.22, 2.93, 2.63, and 2.30 Å, respectively. The hydrophobic bonds between ALA280, ILE344, ALA310, ILE344, and ALA280 have distances of 4.76, 4.70, 3.77, 3.66, and 3.46 Å, respectively. The results show a resemblance in hydrogen bonding between A1 and the native ligand and bempedoic acid, representing GLY380 and ARG378. A1 is connected to the binding side by 14 hydrogen bonds. The NH group on the residue acts as a hydrogen donor, binding to the O atom on A1 as a hydrogen acceptor, specifically ALA280, GLY309, ALA310, ILE344, and ASN349. The H atom on A1 acts as a hydrogen donor, binding to the O atom on the residue as a hydrogen acceptor, which is ASN346, MET278, GLY342, GLY380, ARG378, ASN346, ARG378. The H atom on the residue acts as a hydrogen donor,

binding to the O atom on A1 as a hydrogen acceptor, especially SER308, and ARG379.

A2 binding ACC forms 10 hydrogen bonds: ASN679, PHE704, TRP681, GLU671, ARG281, ARG277, ARG277, ASN599, GLU593, PRO590. The bond lengths are 2.39, 2.24, 1.76, 1.69, 2.31, 2.27, 2.95, 3.00, 2.84, 1.84 Å, respectively. Hydrophobic bonds between VAL648, PHE704, TRP681, ILE270, VAL273, LYS274, LYS274, and MET594 have distances of 5.28, 5.13, 4.38, 4.73, 4.46, 4.59, 5.12, and 4.67 Å, respectively. The data obtained show a similarity of hydrogen bonds between the natural ligand and A2, namely at residue ARG277, and with Firsocostat, which is ARG 281. A2 is linked via a binding site with ten hydrogen bonds. The hydrogen donor H atom on A2 binds to the hydrogen acceptor O atom on the residue, which is ASN679, PHE704, PRO590, GLU671, and GLU593. The O atom on A3 acts as a hydrogen acceptor, binding to the H atom on the residue as a hydrogen donor, especially ARG281, TRP681, ARG277, ARG277, and ASN599.

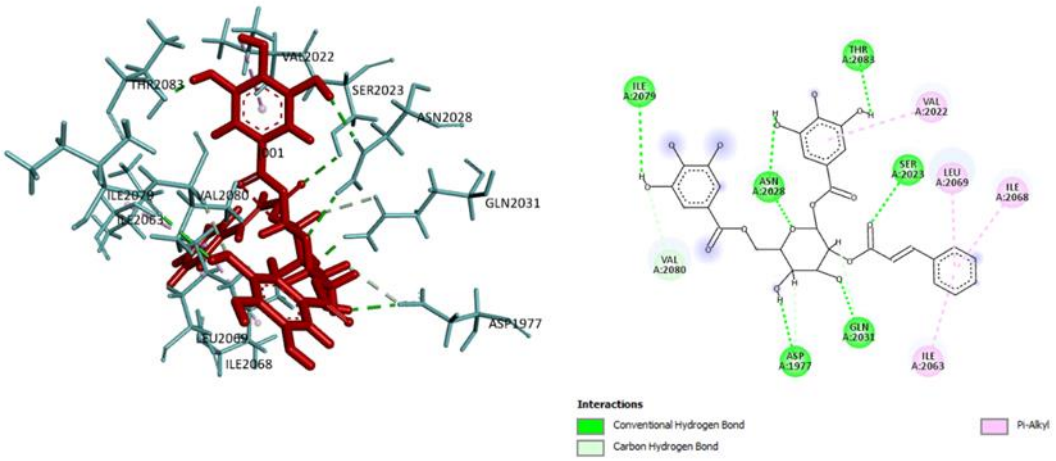

Figure 4. 2D and 3D ligan (A3)-target interactions at binding site of FASN (8GKC)

A3 binding FASN has ten hydrogen bonds from ILE2079, VAL2080, ASN2028, ASP1977, GLN2031, GLN2031, SER2023, and THR2083 with sequential bond distances of 2.70, 2.45, 2.30, 2.38, 2.29, 2.97, 1.84, 2.74, 2.39, 1.94 Å, repsectively. The hydrophobic bonds from VAL2022, LEU2069, ILE2068, and ILE2063 have subsequently bond distances of 4.48, 5.04, 4.50, and 4.26, respectively. The results show that amino acid residues in A3 are comparable to those in the native ligand (GLN2031), orlistat (ASN2028). A3 is coupled to the binding site via ten hydrogen bonds. The H atom of the OH group on A3 works as a hydrogen donor, whereas the O atoms of residues ILE2079, ASN2028, THR2083, and ASP1977 serve as hydrogen acceptors. The O atom on A3 works as a hydrogen acceptor, connecting with the H atoms of ASN2028, SER2023, GLN2031, and VAL2080, which act as hydrogen donors.

A4 binding SCD1 contains nine hydrogen bonds with GLN147, THR261, ASN265, ASN148, TRP153, PHE146, PHE146, HIS157, and THR261 bond distances of 2.91, 2.35, 2.20, 2.25, 1.97, 2.75, 2.98, 2.62, 2.54 Å, respectively. There are 12 hydrophobic bonds: GLN147, TRP153, TRP153, HIS120, TRP153, TRP184, LEU185, TRP153, TRP184, TRP262, LEU185, VAL264 with bond distances of 2.85, 3.84, 4.98, 5.49, 5.08, 4.91, 5.37, 5.11, 4.85, 5.37, 4.84, 4.13 Å, respectively. The results show a residue similarity between A4 and the native ligand, ASN148. The H atom of the hydroxyl group on A4, as a hydrogen donor, binds to the O atom, acting as a hydrogen acceptor on residues PHE146, PHE146, ASN148, and TRP153. As a hydrogen acceptor O atom on the C=O group binds to the H atom of residue THR261, GLN147 as a hydrogen donor. The H atom on residues ASN265 and HIS175 acts as a hydrogen donor and binds to the O atom on A4, which acts as a hydrogen acceptor.

A5 binding HMGCR formed six hydrogen bonds: ALA751, ALA751, ALA856, GLU559, GLU559, and GLY560, with bond lengths of 1.89, 2.37, 2.01, 2.11, 1.82, and 1.96Å, respectively. A5 enhanced hydrophobic interactions with ALA856, LEU853, and HIS752 at distance of 4.60 to 5.32 Å. The interaction between the ligand and protein produces a single amino acid residue, GLU559, similar to A5. This residue activates the HMGCR enzyme. Glutamate residues can absorb hydroxyl radical peptides and exhibit antioxidant bioactivity [59]. A5 shows six hydrogen bonds with the site. Six hydrogen bonds connect A5 and the location. The H atom in the ligand works as a hydrogen donor,

interacting with the O atom in the amino acid residue, which acts as a hydrogen acceptor.

3.3. Lipinski rule of five ADMET analysis

The results of the Lipinski rule of five are shown in Table 3. The only compound that matches Lipinski's rule is A4, which has a molecular weight of less than 500 Da and an H-bond acceptor of less than 10. Other compounds violate the rules with Lipinski's rules. This is due to the complicated structures of A1, A2, A3, and A5, which result in a significant mass for each a compound. Moreover, the presence of glycosides in the molecule increases the number of OH groups or hydrogen bonding. If too many hydrogen bonds exist, the drug structure may become overly reactive and unstable.

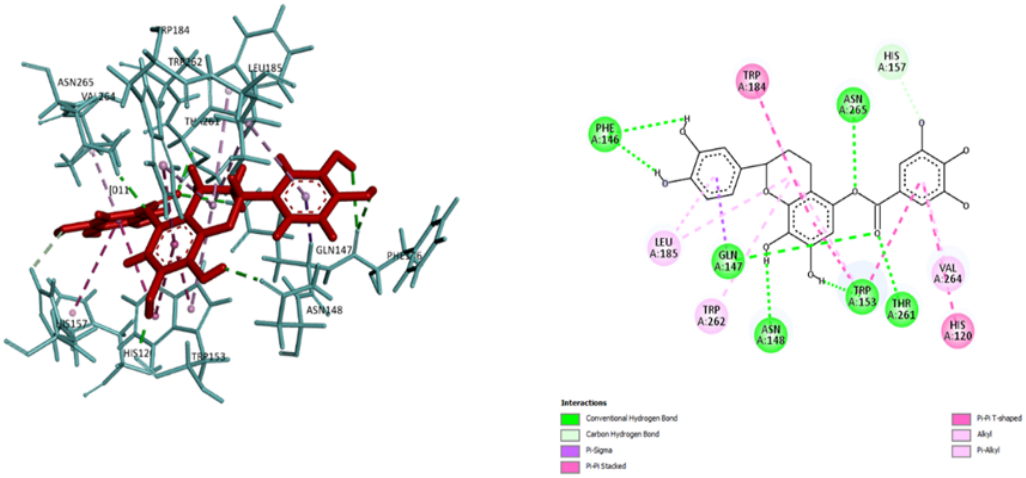

Figure 5. 2D and 3D ligan (A3)-target interactions at binding site of SCD1 (4ZYO)

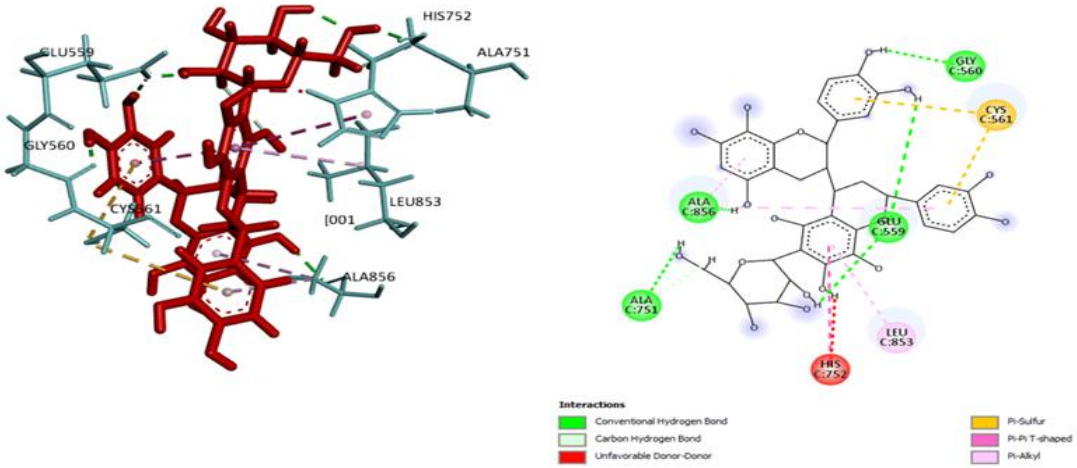

Figure 6. 2D and 3D ligan (A5)-target interactions at binding site of HMGCR (1HW9)

Table 3. Lipinski rule of five

Compound	Mass	H-Bond Donor	H-Bond Acceptors	Log P
A1	614 Da	11	16	-2.70
A2	566 Da	6	11	2.42
A3	614 Da	8	15	1.00
A4	442 Da	7	10	2.91
A5	740 Da	14	17	-1.02

Table 4. ADMET properties

Compound	BA score	GI	BBB	LD_{50}	Toxicity Class	Hepatotoxicity	Cytotoxicity
A1	0.17	Low	No	2500	5	Inactive	Inactive
A2	0.17	Low	No	4000	5	Inactive	Inactive

A3	0.17	Low	No	5000	5	Inactive	Inactive
A4	0.35	Low	No	1000	4	Inactive	Inactive
A5	0.17	Low	No	2500	5	Inactive	Inactive

In table 4. The ADMET properties show that A1, A2, A3, and A5 compounds have the GI of all drugs with low activity, and all compounds lack BBB action. There is toxicology prediction data. The parameters evaluated include LD_{50}, toxicity class prediction, hepatotoxicity, and cytotoxicity. The LD_{50} of compounds relates to its ability to generate adverse effects within a short time following exposure. The lower the LD_{50}, the more potentially dangerous it is. The shown toxicity class is the duration of the risk and its effect on organisms, defined by class 1–6. The smaller the class, the more toxic it is. A1, A2, A3, A4, and A5 have a fairly good or non-toxic LD_{50}, namely >1000 mg/kg, and a predicted toxicity class in the range 4-5. These compounds are also inactive for hepatotoxicity and cytotoxicity, so they are safe to use.

A4 compounds 3-O-galloylepicatechin have good binding activity on each enzyme target. After Lipinski rule and ADMET analysis, this compound is predicted to be potentially safe as an oral drug.

4. Conclusions

The study accurately predicted the effectiveness of the bioactive compounds in the Rheum genus using molecular docking simulation. These results A1, A2, A3, A4, and A5 are predicted to have good binding potential to their respective targets that can inhibit steatohepatitis., by enzyme ACLY, ACC, FASN, SCD1, and HMGCR, respectively. Predicted ADMET properties indicated all compounds met some parameters of pharmacokinetics and toxicity, and just 3-O-galloylepicatechin met some parameters of Lipinski rule. Molecular dynamics simulation needs to be performed to validate the conclusions obtained from the current work. Further investigations required to advance the development of a novel pharmaceutical or drug candidate for steatohepatitis include in-vitro tests, in-vivo tests, and clinical trials.

ACKNOWLEDGEMENT

This work was supported by grants from National Research and Innovation Agency (BRIN) and Institute of Education Fund Management (LPDP) with scheme Research and Innovation for Advanced Indonesia (RIIM) (No. 82/II.7/HK/2022).

References

[1] Eilam Y, Pintel N, Khattib H, Shagug N, Taha R, Avni D, Regulation of Cholesterol Metabolism by Phytochemicals Derived from Algae and Edible Mushrooms in Non-Alcoholic Fatty Liver Disease, International Journal of Molecular Sciences 23 (2022) 13667.

[2] C. D. Byrne and G. Targher, NAFLD: A multisystem disease, Journal of Hepatology 62 (1) (2015) S47-S64.

[3] H. Devarbhavi, S. K. Asrani, J. P. Arab, Y. A. Nartey, E. Pose, and P. S. Kamath, Global burden of liver disease, Journal of Hepatology 79 (2) (2023) 516-537.

[4] P. Bedossa, Pathology of non-alcoholic fatty liver disease, Liver Int 37 (1) (2017) 85-89.

[5] Grander C, Grabherr F, Tilg H, Non-alcoholic fatty liver disease: pathophysiological concepts and treatment options. Cardiovasc Res 119 (9) (2023) 1787-1798.

[6] Imamura F, Fretts AM, Marklund M, Ardisson Korat AV, Yang WS, Lankinen M et al, Fatty acids in the de novo lipogenesis pathway and incidence of type 2 diabetes: A pooled analysis of prospective cohort studies, PLOS Medicine. 17 (6) (2020) e1003102.

[7] Strable MS, Ntambi JM, Genetic control of de novo lipogenesis: role in diet-induced obesity, Crit Rev Biochem Mol Biol 45 (3) (2010) 199-214.

[8] Softic S, Cohen DE, Kahn CR, Role of Dietary Fructose and Hepatic De Novo Lipogenesis in Fatty Liver Disease, Dig Dis Sci, 61 (5) (2016) 1282-93.

[9] Song Z, Xiaoli AM, Yang F, Regulation and Metabolic Significance of De Novo Lipogenesis in Adipose Tissues, Nutrients 10 (10) (2018) 1383.

[10] Jiang, SY., Li, H., Tang, JJ. et al, Discovery of a potent HMG-CoA reductase degrader that eliminates statin-induced reductase accumulation and lowers cholesterol. Nat Commun 9 (2018) 5138.

[11] Reith, Christina et al, Effect of statin theraphy on muscle symptoms: an individual participant data meta-analysis of large scale, ranomised, double-blind trials. The Lancet 400 (10355) (2022) 832-845.

[12] A. Ghorbani, M. S. Amiri, and A. Hosseini. Pharmacological properties of Rheum turkestanicum Janisch. Heliyon. 5 (6) (2019).

[13] M. Yang, X Li, X Zeng, Zhimin Ou, M Xue, D Gao, S Liu, Xuejun Li, and Shuyu Yang. Rheum palmatum L. Attenuates High Fat Diet-Induced Hepatosteatosis by Activating AMP-Activated Protein Kinase. American Journal of Chinese Medicine 44 (3) (2016) pp. 551–564.

[14] A. K. Shakya. Drug-induced hepatotoxicity and hepatoprotective medicinal plants: A review. Association of Pharmaceutical Teachers of India. (2020).

[15] H Liu, M Chen, Hao Yin, Pei Hu, Yangyang Wang, F Liu, X Tian, C Huang. Exploration of the hepatoprotective chemical base of an orally administered herbal formulation (YCHT) in normal and CCl4-intoxicated liver injury rats. Part 1: Metabolic profiles from the liver-centric perspective, Journal of Ethnopharmacology 237 (2019) 81-91.

[16] M.-A.-R. Hadjzadeh, Z. Rajaei, E. Khodaei, M. Malek, and H. Ghanbari, Rheum turkestanicum rhizomes possess anti-hypertriglyceridemic, but not hypoglycemic or hepatoprotective effect in experimental diabetes, Avicenna Journal of Phytomedicine 7 (1) (2017) 1-9.

[17] Firdayani, A. Riswoko, and I. Helianti, Inhibition of SARS-Cov-2 proteases by medicinal plant bioactive constituents: Molecular docking simulation, IOP Conference Series: Earth and Environmental Science 976 (2022).

[18] Ghazwani MY, Bakheit AH, Hakami AR, Alkahtani HM, Almehizia AA, Virtual Screening and Molecular Docking Studies for Discovery of Potential RNA-Dependent RNA Polymerase Inhibitors, Crystals 11 (5) (2021) 471.

[19] Maliehe TS, Tsilo PH, Shandu JS, Computational Evaluation of ADMET Properties and Bioactive Score of Compounds from Encephalartos ferox, Pharmacognosy Journal 12 (6) (2020) 1357-1362.

[20] Iresha, Muthia Rahayu; Firdayani, Firdayani; Sani, Agam Wira; Karimah, Nihayatul; Listiana, Shelvi; Tanasa, Irfansyah Yudhi; Sartono, Arief; and Masyita, Ayu, Machine Learning Model and Molecular Docking for Screening Medicinal Plants as HIV-1 Reverse Transcriptase Inhibitors, Karbala International Journal of Modern Science 10 (1) (2024) Article 7.

[21] B. Santoso, Pengaruh Volume Gridbox pada Docking Senyawa dalam Stelechocarpus burahol terhadap Protein Homolog antiinflamasi TRPV, University Research Colloqium (2017), ISSN: 2047-9189.

[22] A. K. Ghosh and S. Gemma, "Front Matter," in Structure-Based Design of Drugs and Other Bioactive Molecules, Wiley (2014).

[23] Kufareva I, Abagyan R, Methods of protein structure comparison, Methods Mol Biol 857 (2012) 231-57.

[24] M. R. Fadhil Pratama, H. Poerwono, and S. Siswodihardjo, Introducing a two-dimensional graph of docking score difference vs. similarity of ligand-receptor interactions, Indonesian J Biotechnol 26 (1) (2021) 54–60.

[25] K. Brusselmans, R. Vrolix, G. Verhoeven, and J. V. Swinnen, Induction of cancer cell apoptosis by flavonoids is associated with their ability to inhibit fatty acid synthase activity, Journal of Biological Chemistry 280 (7) (2005) 5636–5645.

[26] Aranaz P, Navarro-Herrera D, Zabala M, Romo-Hualde A, López-Yoldi M, Vizmanos JL, Milagro FI, González-Navarro CJ, Phenolic Compounds Reduce the Fat Content in Caenorhabditis elegans by Affecting

Lipogenesis, Lipolysis, and Different Stress Responses, Pharmaceuticals (Basel) 30; 13 (11) (2020) 355.

[27] D. Kesuma, S. Siswandono, B. T. Purwanto, and S. Hardjono, Uji in silico Aktivitas Sitotoksik dan Toksisitas Senyawa Turunan N-(Benzoil)-N'- feniltiourea Sebagai Calon Obat Antikanker, Journal of Pharmaceutical Science and Clinical Research 3 (1) (2018).

[28] Yoshika K, Gen I, Itsuo N, Tannins and Related Compounds. XLV. Rhubarb. (5). Isolation and Characterization of Flavan-3-ol and Procyanidin Glucosides, Chem. Pharm. Bull 34 (8) (1986) 3208-3222.

[29] Yoshika K, Gen I, Itsuo N. Studies on Rhubarb (Rhei Rhizoma). VI. Isolation and Characterization of Stillbenes. Cherm. Pharm. Bull 32 (9) (1984) 3501-3517.

[30] E. A. Haddock, R. K. Gupta, S. M. K. Al-Shafi, E. Haslam, and D. Magnolato, The metabolism of gallic acid and hexahydroxydiphenic acid in plants. Part 1. Introduction. Naturally occurring galloyl esters, J Chem Soc Perkin 1, pp. (1982). 2515–2524.

[31] S. K. Agarwal, S. S. Singh, V. Lakshmi, S. Verma, and S. Kumar, Chemistry and Pharmacology of Rhubarb (Rheum species)-A Review, Journal of Scientific & Industrial Research 60 (2001) 1-9.

[32] Satoshi M, Gen I, Itsuo N, Tannins and Related Compounds. XXXIX. Procyanidin C-Glucosides and an Acylated Flavan-3-ol Glucoside from the Barks of Cinnamomum cassia BLUME and C.obtusifolium NESS, Chem. Pharm. Bull 34 (2) (1986) 643-649.

[33] Y. Luo, Y. Jian, Y. Liu, S. Jiang, D. Muhammad, and W. Wang, Flavanols from Nature: A Phytochemistry and Biological Activity Review 27 (3) (2022) 719.

[34] H. C. da Silva, F. das C. L. Pinto, A. F. de Sousa, O. D. L. Pessoa, M. T. S. Trevisan, and G. M. P. Santiago, Chemical constituents and acetylcholinesterase inhibitory activity from the stems of Bauhinia pentandra, Nat Prod Res, 35 (23) (2021) 5277–5281.

[35] Baek, JA., Son, YO., Fang, M, Y Jae Lee, H-Kwon Cho, Wan Kyunn Whang, and J-Chae Lee, Catechin – 7 – O – β – d - glucopyranoside scavenges free radicals and protects human B lymphoma BJAB cells on H_2O_2-mediated oxidative stress, Food Sci Biotechnol **20**, (2011) 151–158.

[36] A. Usman, V. Thoss, and M. N Alam, Isolation and Identification of Flavonoids Components from Trichilia emetica Whole Seeds, Journal of Natural Products and Resources 4 (2) (2018). 179–181.

[37] Costabile G, Della Pepa G, Salamone D, Luongo D, Naviglio D, Brancato V, Cavaliere C, Salvatore M, Cipriano P, Vitale M, et al, Reduction of De Novo Lipogenesis Mediates Beneficial Effects of Isoenergetic Diets on Fatty Liver: Mechanistic Insights from the MEDEA Randomized Clinical Trial, Nutrients 14 (10) (2022) 2178.

[38] Granchi C, ATP citrate lyase (ACLY) inhibitors: An anti-cancer strategy at the crossroads of glucose and lipid metabolism, Eur J Med Chem 157 (2018) 1276-1291.

[39] M. R. Morrow et al., Inhibition of ATP-citrate lyase improves NASH, liver fibrosis, and dyslipidemia, Cell Metab 34 (6) (2022) 919-936.

[40] O. Yizhar and J. S. Wiegert, Designer Drugs for Designer Receptors: Unlocking the Translational Potential of Chemogenetics, 40 (6) (2019) 362-364.

[41] K. V. Sanjay, S. Vishwakarma, B. R. Zope, V. S. Mane, S. Mohire, and S. Dhakshinamoorthy, ATP citrate lyase inhibitor Bempedoic Acid alleviate long term HFD induced NASH through improvement in glycemic control, reduction of hepatic triglycerides & total cholesterol, modulation of inflammatory & fibrotic genes and improvement in NAS score, Current Research in Pharmacology and Drug Discovery 2 (2021) 100051.

[42] Y. Wang, W. Yu, S. Li, D. Guo, J. He, and Y. Wang, Acetyl-CoA Carboxylases and Diseases 12 (2022) 836058.

[43] Gao YS, Qian MY, Wei QQ, Duan XB, Wang SL, Hu HY, Liu J, Pan CY, Zhang SQ, Qi LW, Zhou JP, Zhang HB, Wang LR, WZ66, a novel acetyl-CoA carboxylase inhibitor, alleviates nonalcoholic steatohepatitis (NASH) in mice. Acta Pharmacol Sin 41 (3) (2020) 336-347.

[44] Eric J. Lawitz, Kelvin W. Li et al, Elevated de novo lipogenesis, slow liver triglyceride turnover, and clinical correlations in nonalcoholic steatohepatitis patients. J Lipid Res 63 (9) (2022).

[45] Li EQ, Zhao W, Zhang C, Qin LZ, Liu SJ, Feng ZQ, Wen X, Chen CP, Synthesis and anti-cancer activity of ND-646 and its derivatives as acetyl-CoA carboxylase 1 inhibitors. Eur J Pharm Sci 137 (2019) 105010.

[46] N. Alkhouri, E. Lawitz, M. Noureddin, R. DeFronzo, and G. I. Shulman, GS-0976 (Firsocostat): an investigational liver-directed acetyl-CoA carboxylase (ACC) inhibitor for the treatment of non-alcoholic steatohepatitis (NASH), Expert Opin Investig Drugs 29 (2) (2020). pp. 135–141.

[47] Postic C, Girard J, Contribution of de novo fatty acid synthesis to hepatic steatosis and insulin resistance: lessons from genetically engineered mice, J Clin Invest. 118 (3) (2008) 829-38..

[48] M. O'Farrell et al, FASN inhibition targets multiple drivers of NASH by reducing steatosis, inflammation and fibrosis in preclinical models 12 (1) (2022).

[49] R Loomba, R Mohseni, K et al, TVB-2640 (FASN Inhibitor) for the Treatment of Nonalcoholic Steatohepatitis: FASCINATE-1, a Randomized, Placebo-Gastroenterology 161 (5) (2021) 1475-1486.

[50] Sankaranarayanapillai, M., Zhang, N, Baggerly, K.A, Gelovani, J.G, Metabolic shifts induced by fatty acid synthase inhibitor orlistat in non-small cell lung carcinoma cells provide novel pharmacodynamic biomarkers for positron emission tomography and magnetic resonance spectroscopy, Mol. Imaging Biol 15 (2013) 136–147.

[51] Chen L, Ren J, Yang L, Li Y, Fu J, Li Y, Tian Y, Qiu F, Liu Z, Qiu Y, Stearoyl-CoA desaturase-1 mediated cell apoptosis in colorectal cancer by promoting ceramide synthesis 6 (2016) 19665.

[52] Bhattacharya D., Basta B., Mato J.M., Craig A., Fernández-Ramos D., Lopitz-Otsoa F., Tsvirkun D., Hayardeny L., Chandar V., Schwartz R.E., et al, Aramchol downregulates stearoyl CoA-desaturase 1 in hepatic stellate cells to attenuate cellular fibrogenesis. JHEP Rep 3 (2021) 100237.

[53] Petroff AB, Weir RL, Yates CR, Ng JD, Baudry J, Sequential Dynamics of Stearoyl-CoA Desaturase-1(SCD1)/Ligand Binding and Unbinding Mechanism: A Computational Study, Biomolecules 30; 11 (10) (2021) 1435.

[54] D. Bhattacharya et al, Aramchol downregulates stearoyl CoA-desaturase 1 in hepatic stellate cells to attenuate cellular fibrogenesis, JHEP Reports 3 (3) (2021).

[55] F. W. B. Sanders and J. L. Griffin, De novo lipogenesis in the liver in health and disease: More than just a shunting yard for glucose. Biological Reviews 91 (2) (2016) 452–468.

[56] S. Suganya, B. Nandagopal, and A. Anbarasu, Natural Inhibitors of HMG-CoA Reductase An Insilico Approach Through Molecular Docking and Simulation Studies. J Cell Biochem 118 (1) (2017) 52–57.

[57] Van Rooyen DM, Farrell GC, SREBP-2: a link between insulin resistance, hepatic cholesterol, and inflammation in NASH. J Gastroenterol Hepatol 26 (5) (2011). 789-92.

[58] Nagashima S, Yagyu H, Ohashi K, Tazoe F, Takahashi M, Ohshiro T, Bayasgalan T, Okada K, Sekiya M, Osuga J, Ishibashi S, Liver-specific deletion of 3-hydroxy-3-methylglutaryl coenzyme A reductase causes hepatic steatosis and death. Arterioscler Thromb Vasc Biol 32 (8) (2012) 1824-31.

[59] Li X, Guo M, Chi J, Ma J, Bioactive Peptides from Walnut Residue Protein, Molecules 25 (6) (2020) 1285.